SAND2011-5051C

# CONTROLLING FEED ELECTRON FLOW IN MITL-DRIVEN RADIOGRAPHIC DIODES

**David B. Seidel**[ξ]**, Timothy D. Pointon, and Bryan V. Oliver**
*Sandia National Laboratories*[*]*, PO Box 5800, Albuquerque, NM 87185-1152 USA*

*Abstract*

The electrons flowing in a coaxial magnetically insulated transmission line (MITL), if allowed to flow uncontrolled into a radiographic electron diode load, can have an adverse impact on the performance of the system. Total radiation dose, impedance lifetime, and spot quality (size, shape, position, and stability) can all be affected. Currently available approaches to deal with this problem typically require a large volume in the vicinity of the electron diode load. For applications where this volume is not available, an alternate method of controlling the feed electrons is needed. In this paper, we will investigate various ideas for dealing with this issue and present results showing the properties of the various schemes investigated, and compare the relative merits of any that prove viable.

## I. INTRODUCTION

The Radiographic Integrated Test Stand (RITS) at Sandia National Laboratories is used for advanced radiography applications. In its current form (RITS-6), it consists of 6 pulse-forming lines (PFL) feeding six induction cavities which are joined in series by a 51 Ω MITL. This system can deliver 7-11 MV at 150-200 kA in a 75-ns pulse.

The electrons flowing in the coaxial MITL, if allowed to flow uncontrolled into the radiographic electron diode load, can have an adverse impact on the performance of the system. Total radiation dose, impedance lifetime, and spot quality (size, shape, position, and stability) can be all affected [1]. One common approach to keeping such feed electrons out of the diode region involves greatly increasing the radius of the MITL's outer (anode) electrode near the diode and adding a large, rounded field shaper to the load end of the inner cathode conductor, forcing these electrons to be lost to the to the anode outside the diode itself [2]. This configuration (see Fig. 1) is referred to as the "knob and dustbin". While this approach can be quite successful, there is an inductance penalty that reduces the current that can be delivered to the load and it requires a large volume in the vicinity of the load. For applications where this volume is not available, an alternate method of controlling the feed electrons is needed.

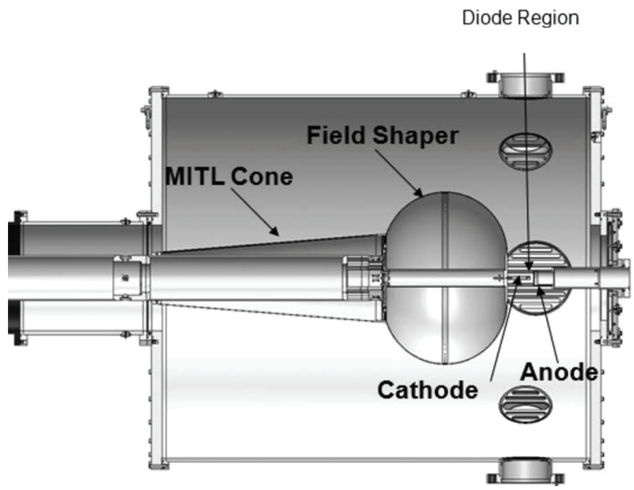


**Figure 1.** RITS-6 load configuration showing large radius chamber (dustbin) and the spherical field shaper (knob). Taken from Ref. 1.

In this paper, we will investigate various ideas for dealing with this issue. For example, one could consider the effect of a solenoidal magnetic field at or near the end of the MITL on the electron flow. Such fields have been successfully used in other devices, such as ion diodes [3] and plasma opening switches [4], to control the flow of electrons. These fields could be produced using the MITL current directly by adding one or more field coils in series with the MITL circuit, or through coils that are pulsed using a separate power supply, possibly on a longer timescale.

We will present results showing the properties of the various schemes investigated, and compare the relative merits of any that prove viable.

[ξ] Email: dbseide@sandia.gov
[*] Sandia National Laboratories is a multi-program laboratory managed and operated by Sandia Corporation, a wholly owned subsidiary of Lockheed Martin Corporation, for the U. S. Department of Energy's National Nuclear Security Administration under contract DE-AC04-94AL85000.

## II. USING MAGNETIC FIELD TO CONTROL FEED ELECTRONS

The magnetic field produced by azimuthally-wrapped coils can have a significant effect on electrons in MITL systems. Electrons are affected in two basic ways: first, field lines connecting feed electrodes can carry electrons to the anode, and second, electrons crossing net magnetic flux are constrained outside some minimum radius.

If an electron's energy and canonical angular momentum are conserved,

$$\left(\frac{\Delta\Psi}{r_a}\frac{e}{mc}\right)^2 = \left(\frac{e\Phi(\mathbf{r})}{mc^2}+1\right)^2 - 1 - \gamma\left(\beta_z^2+\beta_r^2\right), \qquad (1)$$

where $\Psi(\mathbf{r}) = rA_\theta(\mathbf{r})$ is the magnetic stream function, $\Phi$ is the scalar potential ($\Phi_c = 0$), and $\Delta\Psi = \Psi(\mathbf{r}_c) - \Psi(\mathbf{r}_a)$. $\boldsymbol{\beta} = \mathbf{v}/c$ is the electron's normalized velocity, and $\mathbf{r}_c$ and $\mathbf{r}_a$ are the electron's cathode emission and anode loss locations, respectively. Since the $\beta^2$ terms in (1) are always positive, a minimum electron radius can be obtained:

$$r_a \geq \frac{e}{mc}\Delta\Psi\left[\left(\frac{eV}{mc^2}+1\right)^2 - 1\right]^{-1/2}. \qquad (2)$$

### *A. Magnetic Field Coils in Series with MITL*

One of the two common ways to add a magnetic field to a pulsed-power device is to include a coil in series with the MITL circuit so that it is energized by the current carried by the MITL. Fig. 2 shows such a coil from a triggered plasma opening switch. The helical winding in

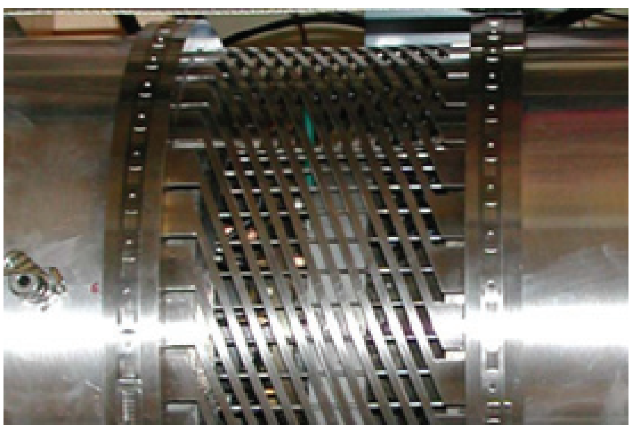

**Figure 2.** Series field coil from a triggered plasma opening switch system.

the outer conductor of the coaxial MITL generates a solenoidal field. Also note that a purely axial winding on the inner conductor allows flux from the solenoidal field to penetrate through the inner conductor.

To explore using such a coil in a low-volume RITS front-end, we considered a geometry in which the MITL inner and outer radii, 8 cm and 19 cm, respectively (shown at far left in Fig. 1), continued uniformly all the way to the diode. The magnetic field was computed using

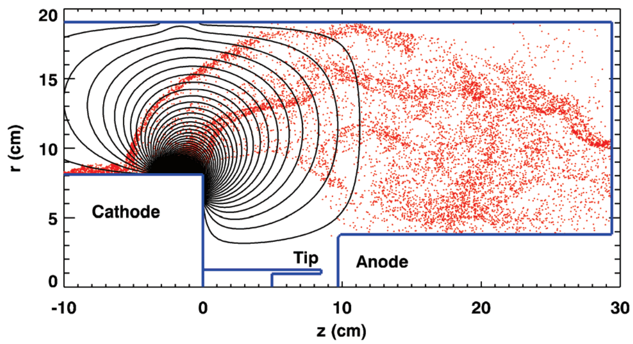


**Figure 3.** Simulation geometry showing magnetic stream lines for a cathode series field coil and snapshot of feed electrons at the time of peak diode voltage and current. Simulation electrons emitted from the $z$ = 0 surface and the cathode tip are not shown here.

the Atheta code [5], placing coils at the cathode radius within a few centimeters of the end of the cathode stalk. Flux was allowed to penetrate 2 cm radially inward at the end of the cathode stalk, corresponding to radial coil vanes in a field coil. Using this field, the Quicksilver electromagnetic particle-in-cell code was used to examine electron flow behavior. The simulation was driven with the input waveform of RITS-6, and operated at ~6 MV and 160 kA. To properly model the details of the diode, ions must be emitted from the anode surface (face) immediately opposite the cathode tip. However, since we are only interested in the behavior of the MITL electrons, we here neglect ions, and instead slightly adjust the anode-cathode gap to reproduce the actual operating impedance of the diode.

Fig. 3 shows this geometry with superimposed magnetic stream lines and snapshot of electron locations at peak power. In order to provide enough flux to keep most of the feed electrons out of the diode region (see Eq. 2), the coil required 120 kA-turns of azimuthal drive current. To achieve this with the available MITL current (160 kA) would require that the vanes of the coil each wrap 1.5π radians. Such a high wrap factor would introduce daunting challenges in designing a coil with adequate mechanical strength.

### *B. Externally-Driven Magnetic Field Coils*

*1) Cathode Coils*

We now modify the geometry shown in Fig. 3 by inserting an externally-pulsed, 12-turn coil in a toroidal-shaped housing, made of a lossy conductor such as stainless steel, as shown in Fig. 4. The magnetic field shown is obtained using Atheta. With this magnetostatic solution, we have effectively assumed the field has entirely diffused through the lossy housing, but has not penetrated the other conductors (e.g., aluminum). This coil has an inductance of 8.1 μH. Using (2), we can select a drive current for the coil such that $\Delta\Psi$ over a large fraction of the coil housing surface will exclude 6 MeV electrons from the interior of the diode ($r$ < ~5 cm). For this coil, the current needed is 10-15 kA.

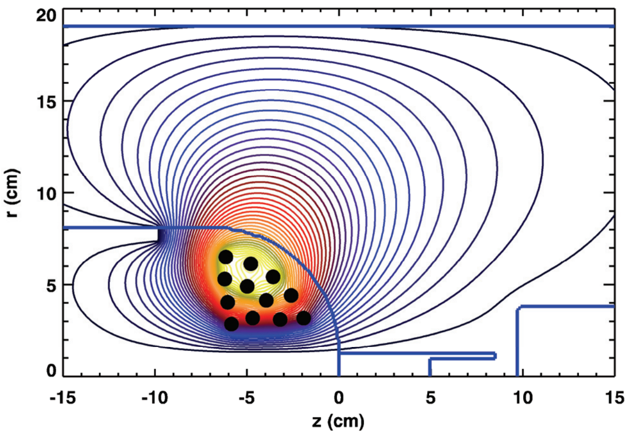


**Figure 4.** Geometry and magnetic stream function for a 12-turn cathode coil system.

A Quicksilver simulation was performed using this geometry and magnetic field, whose amplitude was adjusted consistent with a 12.5 kA coil current. Fig. 5 shows a snapshot of the location of electrons emitted from the MITL feed at a time when the diode voltage and current are near maximum. Note that electrons emitted from the cathode tip (diode electrons) and electrons emitted from the curved surface of the coil housing (face electrons) are not shown. Fig. 6 shows the diode voltage $V_d$ and various current measurements: $I_d$, which measures all electron current striking the anode face (shown in red in Fig. 5), $I_c$, which measures the current emitted from the cathode tip, and $I_{feed}$ and $I_{face}$, which measure the portion of $I_d$ due to feed and face electrons, respectively. Our goal is to minimize these last two currents. The locations of $I_d$ and $I_c$ are indicated in Fig. 5. With this magnetic field amplitude, all feed electrons are kept out of the diode region below ~3.5 MV; at higher voltage, the electrons emitted upstream of the coil are lost to the anode face. Only a small fraction of the face electrons are lost to the anode face due to their non-zero canonical angular momentum.

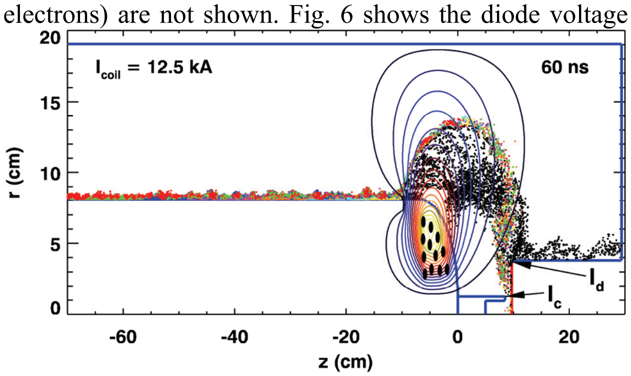


**Figure 5.** Snapshot of feed electrons at 60 ns. Particles are colored by their emission location. Diode and face electrons are not shown. Note aspect *rz* ratio is distorted.

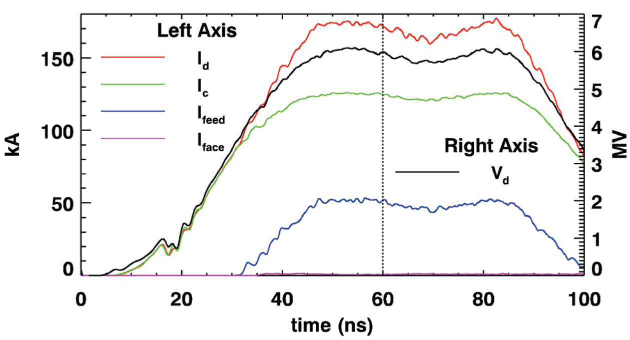


**Figure 6.** Measured currents and diode voltage vs. time for 12.5 kA cathode coil simulation.

If we increase the coil current, the performance can be improved. Figs. 7 and 8 show results of a Quicksilver simulation using a 30 kA coil current. With the increased magnetic field, all feed electrons stay out of the diode region below ~5.2 MV, and the feed current to the anode face is down by more than an order of magnitude. However, there has been a decrease in diode current (~30 kA) and voltage (~0.5 MV), due to increased electron loss in the feed which causes the accelerator to see a somewhat lower impedance. For the intermediate case of a 20 kA coil drive, it was found that (compared to the 12.5 kA case) feed electrons remain out of the diode region below ~4.5 MV, feed current is down by a factor of ~3, and the diode current and voltage are reduced by ~20 kA and ~0.25 MV, respectively.

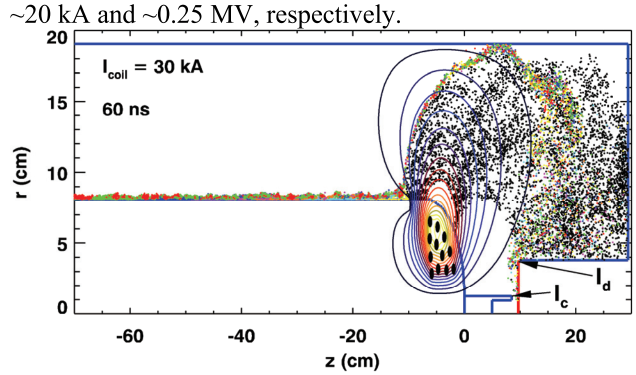


**Figure 7.** Snapshot of feed electrons at 60 ns. Particles are colored by their emission location. Diode and face electrons are not shown. Note aspect *rz* ratio is distorted.

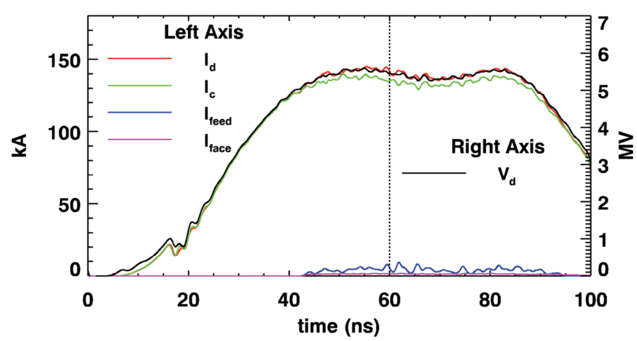


**Figure 8.** Measured currents and diode voltage vs. time for 30 kA cathode coil simulation.

To obtain a crude estimate of the requirements of the external circuit needed to drive this 12-turn coil, we can neglect losses and stray external inductance. With this approximation, we find that a ~200 μF capacitor bank will produce a current pulse that peaks 60 μs after the bank is switched. To obtain a 30 kA peak current, a charging voltage of ~7 kV is needed, corresponding to ~5 kJ initial stored energy.

With the coil configuration we have chosen (see Fig. 4), the anode excludes all flux and consequently the magnetic field lines do not penetrate the anode. It is reasonable to ask whether this is a limiting factor on performance. To test this, several Quicksilver simulations were performed in which a lossy conductor, dubbed an "electron catcher," was inserted on the inner surface of the anode with an inner radius of 15 cm and axial length of 30 cm, as shown in Fig. 9. Also shown in Fig. 9 are the locations of feed electrons for one of those simulations, which used a driving coil current of 16 kA, at a time when diode voltage and current are near maximum. Fig. 10 shows diode voltage and various currents, similar to Figs. 6 and 8, for this same simulation. Essentially all feed and face electrons striking the anode face have been eliminated. However, diode voltage and current have been reduced to ~4.5 MV and ~120 kA, respectively. This is because the insertion of the electron catcher has reduced the self-limited impedance of the MITL, resulting in larger feed losses, which consequently load down the operating voltage. For this coil current (16 kA), an estimate of the voltage and energy requirements of the external coil circuit, using the same approximations, are reduced to ~3.5 kV and ~1.25 kJ.

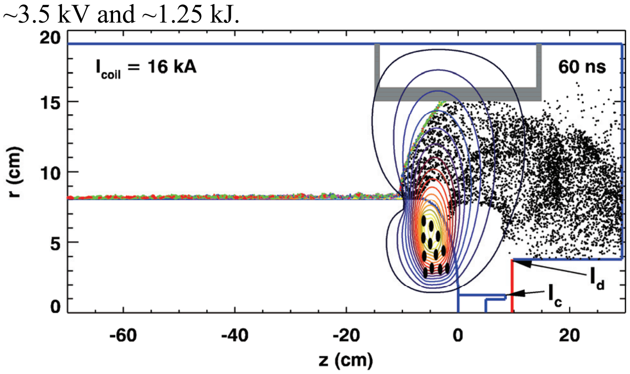


**Figure 9.** Snapshot of feed electrons for geometry with an "electron catcher" (shown in gray). Particles are colored by their emission location. Diode and face electrons are not shown. Note aspect *rz* ratio is distorted.

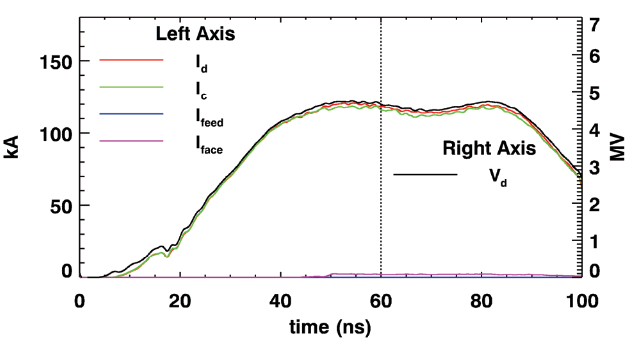


**Figure 10.** Measured currents and diode voltage vs. time for 16 kA cathode coil simulation with an anode "electron catcher."

Another approach that allows magnetic field to penetrate the anode would be to replace some extent of the existing aluminum anode with a lossy insert, or alternately a series field coil with a modest wrap factor (say 1 radian) which could provide ~ 30 kA-turns. Both these approaches would somewhat increase the radius of the system. Both of these approaches were tested, with results in all cases indicating that they produce no significant difference in performance. This leads one to the conclusion that field penetration of the anode does not have a large effect, and the performance of the "electron catcher" described previously was dominated primarily by its reduction of the MITL self-limited impedance.

*2) Anode Coils*

We now modify the geometry shown in Fig. 4 by removing the cathode coil (but keeping the toroidal-shaped cathode face) and inserting an externally-pulsed 22-turn coil, enclosed in a lossy-conductor housing, into the anode, as shown in Fig. 11. Note that the addition of an anode coil necessarily will increase the radius of the overall system. However it is still significantly less than that of the knob-dustbin (Fig. 1) currently used on RITS.

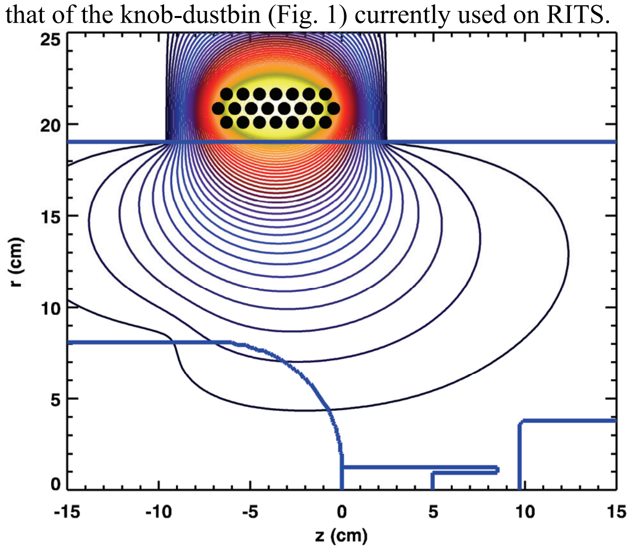


**Figure 11.** Geometry and magnetic stream function for a 22-turn anode coil system. Note diffusion into cathode.

The magnetic field shown in Fig. 11 is obtained using Atheta, again with all the assumptions associated with a magnetostatic solution. Note that we have assumed that this externally-applied field penetrates into some portion of the cathode face structure. This would require that this portion of the cathode be made of a lossy conductor or that it be axially slotted or fluted. This coil has an inductance of 170 μH. Using (2), we can select a drive current for the coil such that electrons emitted over a large fraction of the toroidal surface will exclude 6 MeV electrons from the interior of the diode ($r$ < ~5cm). For this coil, the current needed is 15-25 kA.

Using this geometry, a Quicksilver run with an applied field corresponding to a 15 kA coil current was performed. Fig. 12 shows a snapshot in time of simulation electrons emitted from both the MITL feed and the toroidal cathode face. Fig. 13 shows the corresponding

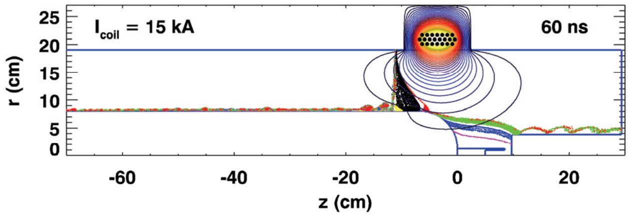


**Figure 12.** Snapshot of feed and face electrons at 60 ns. Particles are colored by their emission location. Diode electrons are not shown.

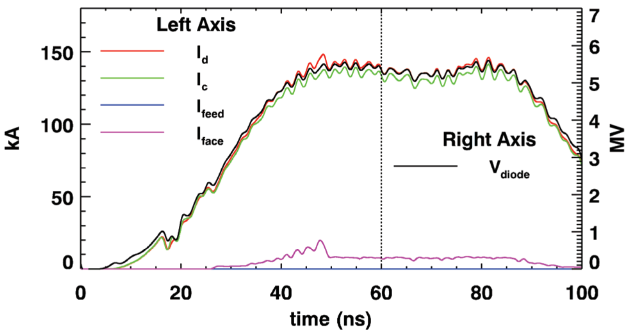


**Figure 13.** Measured currents and diode voltage vs. time for 15 kA anode coil simulation.

voltage and current waveforms. All of the feed electrons are lost outside the diode region over the entire pulse duration. Some of the face-emitted electrons are lost to the anode face. These electrons are emitted at small radius, where one their way to the anode they cross insufficient flux to exclude them from the diode region.

Several more Quicksilver runs were performed using this geometry, gradually increasing the current drive of the coil. At 30 kA, essentially no feed or face electrons reach the anode face over the entire extent of the pulse. However, at this current, and neglecting losses, the energy of the bank driving the coil would need to be ~75 kJ, so actual requirements can be expected to be well over 100 kJ. In addition, to avoid unwanted flux penetration into the aluminum parts of the system (e.g., the cathode tip), the bank capacitance will need to be fairly small, resulting in a very large required charge voltage.

For our simulations, it has been assumed that the cathode face is fabricated and prepared in the same way as the existing knob (see Fig. 1), where electric-field breakdown thresholds as high as 1 MV/cm have been reported [2]. A commonly-used, conservative estimate for this value is 550 kV/cm, which we have used our simulations. If the results of these simulations are examined closely, it is observed that the emission of electrons from the cathode face is actually quite spotty, as can be seen in Fig. 12. In fact, the only locations on the cathode surface that exceed the breakdown threshold are at the small corners that are the inevitable result of fitting a smooth curved surface to a rectilinear grid. At such corners, the electric field is unphysically enhanced due to well-known edge effects. Fig. 14 shows an outline (in black) of the grid-based fit to the cathode face surface, where the corners are clearly visible. It also shows |E| at a time that is representative of peak field strength. Except at the unphysical corners, the field does not exceed the breakdown threshold below some minimum radius (7.3 cm). Consequently, it is reasonable to assume that limiting emission on this portion of the cathode face is justified.

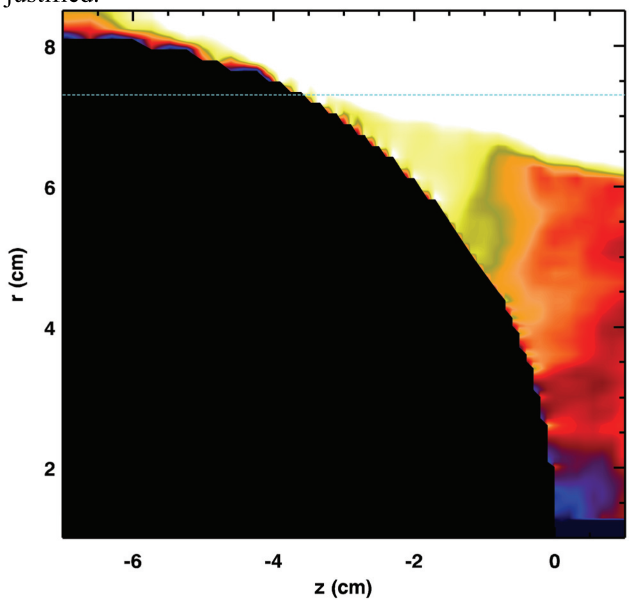


**Figure 14.** |**E**| on cathode face. White indicates |**E**| > 550 MV/cm; all other colors indicate |**E**| < 550 MV/cm. Emission suppressed for *z* < 7.3 cm (dashed cyan line).

To test this, simulations were repeated with emission disabled at positions on the cathode face less than 7.3 cm radius. Figs. 15 and 16 show results using a 13 kA coil current. Unwanted feed and face electron loss to the

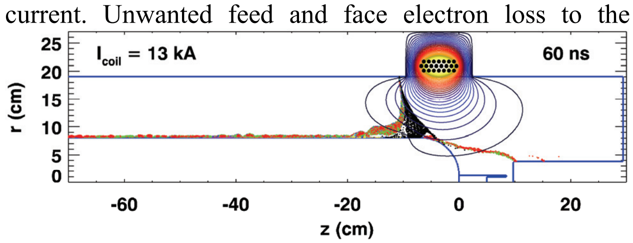


**Figure 15.** Snapshot of feed and face electrons at 60 ns. Particles are colored by their emission location. Diode electrons are not shown. Electron emission suppressed for *r* < 7.3 cm.

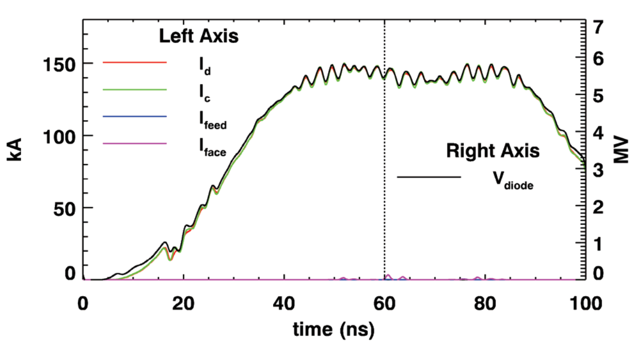


**Figure 16.** Measured currents and diode voltage vs. time for 13 kA anode coil simulation with emission suppressed for *r* < 7.3 cm

anode face is negligible over the entire pulse. Also notice that the penalty in diode voltage and current due to excessive loading of the accelerator is significantly less that for the cathode coil with "electron catcher" configuration (see Fig. 10).

Again we'll use a lossless approximation for the bank requirements to drive this 13 kA anode coil. The required energy is ~15 kJ. There is a tradeoff between the charge voltage and the time to peak current. Table 1 shows some representative values.

**Table 1.** Approximate peak time and required capacitance for 13 kA anode coil system for various charge voltages.

| Charge Voltage (kV) | $t_{peak}$ (μs) | C (μF) |
|---|---|---|
| 20 | 180 | 80 |
| 25 | 140 | 48 |
| 30 | 120 | 33 |

### *C. Tradeoffs of Various Magnetic Control Systems*

Azimuthal coils driven in series with the MITL current can provide magnetic fields without the complication of separate drive circuitry, and without the need for lossy conductors, such as stainless steel, which present issues when at cathode potential due to proton activation at the voltages needed for RITS. However, mechanical issues can be quite significant, particularly with the large winding wrap factors needed for this application.

On the other hand, externally-driven field coils can be pulsed on longer timescales, allowing the magnetic field to penetrate lossy conductors. This allows the tailoring of conductors to precisely shape the field. External coils can be fielded in either the cathode or anode (or even both). We have shown that anode coils require significantly larger energies (by about an order of magnitude) than cathode coils to achieve comparable control of electrons. They also will require more volume since they are positioned outside the MITL anode radius. However, the external circuit connection for a cathode coil must be routed through the accelerator's cathode stalk, introducing more loss and stray inductance as well as significant design complications. The solutions explored in this paper all require that magnetic flux penetrate the cathode. Whereas this requires some portion of the cathode be a lossy conductor for cathode coil systems, with all the attendant activation issues, an anode coil system could also achieve the required flux penetration using an axially-fluted design.

## III. SUMMARY

We have investigated several ideas for controlling the flow of MITL feed electrons in a low-volume front end for the RITS-6 accelerator. By using magnetic fields, these electrons can be kept from striking the anode face of the diode, where they would cause an unwanted increase in the anode spot size of the diode's electron beam. This has been a feasibility study (in contrast to a full engineering design) and consequently much more detailed analysis would be required to bring any of these ideas to fruition. However, some basic findings can be summarized:

- Flux requirements at the voltages of interest are probably too high to use field coils in series with the MITL. Coil windings would require nearly a full turn wrap, presenting significant challenges in engineering a sound mechanical design.
- We have demonstrated that fields applied externally on a longer time scale provide effective solutions and seem to be quite feasible.
- Although cathode coil systems require substantially less energy to drive than anode coil systems, they present other difficulties, including more complicated drive circuitry and proton activation issues. Activation problems might be mitigated with judicious selection of coil housing materials.

Another approach that we have just begun to examine is to attempt to passively control electrons (i.e., without magnetic fields) using purely geometric means. This was the approach for the existing "knob and dustbin" design — we just need to apply it with the constraint of reduced volume. We plan to continue pursuing geometric solutions, as well as perform more detailed analysis and optimization of some of the more promising magnetic-field-based techniques that have been described here.

## IV. REFERENCES


[1] K.D. Hahn, N. Bruner, M.D. Johnston, B.V. Oliver, T.J. Webb, D.R. Welch, S.R. Cordova, I. Crotch, R.E. Gignac, J.J. Leckbee, I. Molina, S. Portillo, J.R. Threadgold, and D. Ziska, IEEE Trans. Plasma Sci. **38**, 2652, 2010.

[2] N. Bruner, T. Genoni, E. Madrid, D. Rose, D. Welch, K. Hahn, J. Leckbee, S. Portillo, B. Oliver, V. Bailey, and D. Johnson, PRST Accel. Beams, **11**, 040401, 2008.

[3] S.A. Slutz, D.B. Seidel, and R.S. Coats, J. Appl. Phys., **61**, 4970, 1987.

[4] M.E. Savage, D.B. Seidel, and C.W. Mendel, Jr., IEEE Trans. Plasma Sci. **28**, 1533, 2000.

[5] J.P. Quintenz, D.B. Seidel, M.L. Kiefer, T.D. Pointon, R.S. Coats, S.E. Rosenthal, T.A. Mehlhorn, M.P. Desjarlais, and N.A. Krall, Laser Part. Beams **12**, 283, 1994.